

Anaerobic oxidation of propane coupled to nitrate reduction by a lineage within the class Symbiobacteriia

Received: 12 April 2022

Accepted: 5 October 2022

Published online: 17 October 2022

 Check for updatesMengxiong Wu^{1,5}, Jie Li^{1,5}, Andy O. Leu², Dirk V. Erler³, Terra Stark⁴, Gene W. Tyson², Zhiguo Yuan¹, Simon J. McIlroy²✉ & Jianhua Guo¹✉

Anaerobic microorganisms are thought to play a critical role in regulating the flux of short-chain gaseous alkanes (SCGAs; including ethane, propane and butane) from terrestrial and aquatic ecosystems to the atmosphere. Sulfate has been confirmed to act as electron acceptor supporting microbial anaerobic oxidation of SCGAs, yet several other energetically more favourable acceptors co-exist with these gases in anaerobic environments. Here, we show that a bioreactor seeded with biomass from a wastewater treatment facility can perform anaerobic propane oxidation coupled to nitrate reduction to dinitrogen gas and ammonium. The bioreactor was operated for more than 1000 days, and we used ¹³C- and ¹⁵N-labelling experiments, metagenomic, metatranscriptomic, metaproteomic and metabolite analyses to characterize the microbial community and the metabolic processes. The data collectively suggest that a species representing a novel order within the bacterial class Symbiobacteriia is responsible for the observed nitrate-dependent propane oxidation. The closed genome of this organism, which we designate as ‘*Candidatus* Alkanivorans nitratreducens’, encodes pathways for oxidation of propane to CO₂ via fumarate addition, and for nitrate reduction, with all the key genes expressed during nitrate-dependent propane oxidation. Our results suggest that nitrate is a relevant electron sink for SCGA oxidation in anaerobic environments, constituting a new microbially-mediated link between the carbon and nitrogen cycles.

A considerable amount of natural gas is generated from deep-sea sediments and hydrocarbon seeps in continental margins and terrestrial ecosystems^{1,2}. Most of the natural gas released is consumed by microorganisms in anoxic zones before the gas diffuses into oxic environments and the atmosphere^{3–5}. Studies of anaerobic oxidation of natural gas have focused on the potent greenhouse gas, methane, as the most abundant component (-60–90%)^{6,7}. However, short chain gaseous alkanes (SCGAs), including ethane, propane, n-butane and *iso*-butane, are also substantial constituents of natural gas (up to -20%)⁸, and are important precursors of ozone and organic aerosols⁹. The global atmospheric emissions of SCGAs are estimated to be 9.2–9.6 Tg yr⁻¹ for ethane,

9.6–10.5 Tg yr⁻¹ for propane, 10 Tg yr⁻¹ for butane and 4.2 Tg yr⁻¹ for *iso*-butane¹⁰.

Anaerobic oxidation of methane (AOM) has been extensively studied and is relatively well understood^{11–17}. Anaerobic methanotrophic archaea (ANME) oxidize methane via the reverse methanogenesis pathway, including the key methyl-CoM reductase (MCR) complex. The ANME shuttle electrons from methane to syntrophic sulfate-reducing bacteria (SRB)^{11,12} or directly to the reduction of nitrate and metal oxides^{13–16}. The bacterium ‘*Candidatus* Methyloirabilis oxyfera’ performs AOM via the “intra-aerobic” methane oxidation pathway using nitrite as the sole electron acceptor¹⁷. Microorganisms likely also couple the oxidation of SCGAs to the reduction of these electron acceptors

A full list of affiliations appears at the end of the paper. ✉ e-mail: simon.mcilroy@qut.edu.au; jianhua.guo@uq.edu.au

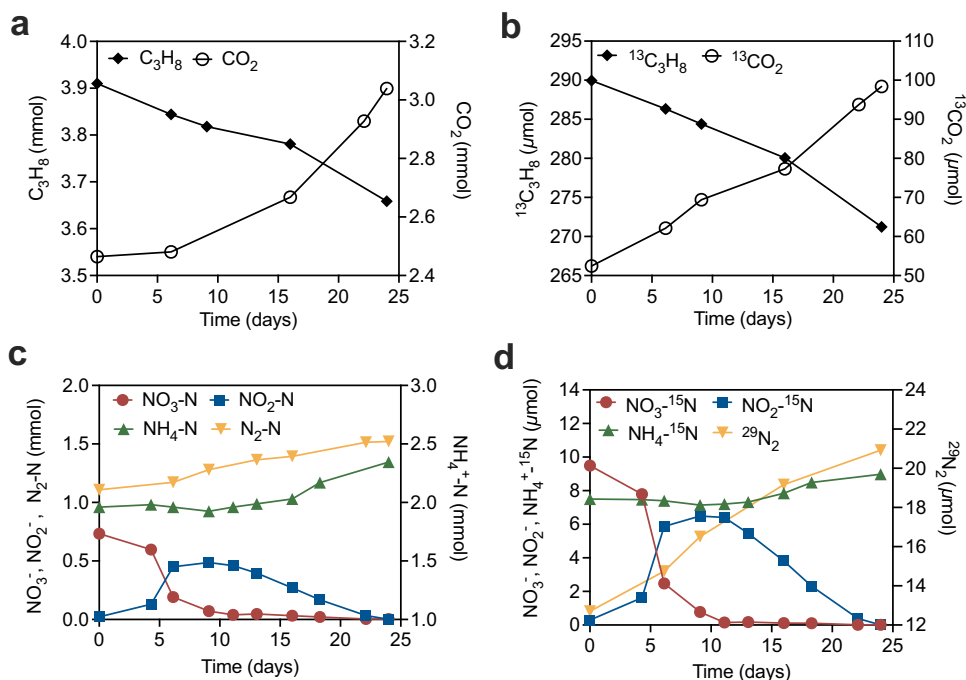


Fig. 1 | Anaerobic oxidation of propane coupled to nitrate reduction by the enrichment culture during the isotope labelling test. a Conversion of C_3H_8 to CO_2 , **b** $^{13}C_3H_8$ to $^{13}CO_2$, **c** NO_3^- to NH_4^+ and N_2 with transitory formation of NO_2^- ,

d $^{15}NO_3^-$ to $^{15}NH_4^+$ and $^{29}N_2$ with transitory formation of $^{15}NO_2^-$. Source data are provided as a Source Data file.

under anoxic conditions¹⁸. ‘*Ca. M. oxyfera*’ were shown capable of oxidizing ethane and propane via the methane monooxygenase, although it is yet to be shown whether these carbon sources support growth¹⁹. To date, sulfate has been the sole electron sink identified to support anaerobic oxidation of SCGAs^{20–25}. The deltaproteobacterial isolate *Desulfosarcina aeriohaga* BuS5 oxidizes propane and butane via the fumarate addition pathway generating alkyl-substituted succinates, a process mediated by alkylsuccinate synthase (ASS)^{20,21}, and directly reduces sulfate to sulphide. An enrichment of the archaeon ‘*Candidatus* Syntrophoarchaeum’ was found to activate butane via butyl-coenzyme M formation, a process catalysed by a divergent MCR, with reducing equivalents channelled to syntrophic SRB partners²³. Similarly, anaerobic ethane oxidation was linked to related ‘*Candidatus* Argoarchaeum ethanivorans’, which also encoded an MCR-like complex and was suggested to form a syntrophic relationship with SRB²². However, an archaeon able to mediate anaerobic propane oxidation directly coupled to sulfate reduction is yet to be identified.

Like sulfate, nitrate is a common electron acceptor in natural ecosystems²⁶, and is used by ANME archaeon ‘*Ca. Methanoperedens nitroreducens*’ for AOM¹⁵. Nitrate reduction coupled to the oxidation of SCGAs (Eq. (1), using propane as an example) is also more thermodynamically feasible compared to the reactions of SCGA oxidation coupled to sulfate reduction ($\Delta G^\circ = -102$ kJ/mol propane)²⁰, but is yet to be linked to any microbial lineage.

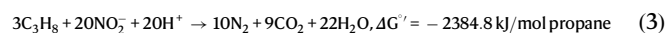
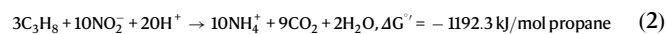
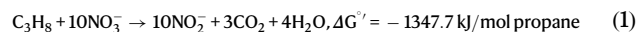
Here we combined mass and electron balance tests, ^{13}C - and ^{15}N -labelling experiments, 16S rRNA gene amplicon sequencing, metabolite analyses and multi-omics approaches to provide evidence that a new bacterial species within the class Symbiobacteriia performs anaerobic oxidation of propane coupled to nitrate reduction.

Results and discussion

Enrichment of a microbial consortia able to couple anaerobic propane oxidation to nitrate reduction

In this study, an anaerobic bioreactor seeded with biomass from a wastewater treatment facility was pulse-fed with propane and nitrate for more than 1000 days. Long-term performance data showed

simultaneous consumption of propane and nitrate, with accumulation of ammonium, dinitrogen gas and transient accumulation of nitrite (Supplementary Fig. 1). No nitrate consumption was observed in the control incubations (without the addition of enrichment culture biomass or propane, Supplementary Fig. 2), suggesting nitrate reduction (to nitrite, ammonium and N_2) coupled to propane consumption in the bioreactor was microbially mediated. To confirm nitrate-dependent anaerobic propane oxidation reaction, and to verify the final products thereof, biomass from the parent reactor was incubated in batch experiments with ^{13}C -labelled propane ($^{13}CH_3^{13}CH_2^{13}CH_3$) and ^{15}N -labelled nitrate ($^{15}NO_3^-$) added to -8% and -1% of the total propane and total nitrate, respectively. The amount of total CO_2 and ^{13}C -labelled CO_2 increased, accompanied by a decrease in C_3H_8 and $^{13}C_3H_8$ (Fig. 1a, b). The ratio (2.42) between the total $^{13}CO_2$ produced (46 μ mol) and total $^{13}C_3H_8$ consumed (19 μ mol) was close to the theoretical stoichiometric ratio of 3:1. The carbon balance suggests that propane was oxidised with CO_2 as the final product. The total NO_3^- consumption (0.73 mmol) was consistent with the combined total N_2 and NH_4^+ production (0.8 mmol) (Fig. 1c). Similarly, the $^{15}NO_3^-$ consumption (9.38 μ mol) was close to the ^{15}N in $^{29}N_2$ (1.1–1.5% of total N_2), $^{30}N_2$ (0.03% of total N_2), and $^{15}NH_4^+$ produced, which amounted to 9.71 μ mol in combination (Fig. 1d). These results confirmed the reduction of nitrate to dinitrogen gas and ammonium. The electrons generated from anaerobic oxidation of propane (AOP, 5.03 mmol) were close to the electron demand for NO_3^- reduction to N_2 and NH_4^+ (5.15 mmol), suggesting electrons generated by AOP were used for denitrification and dissimilatory nitrate reduction to ammonia (DNRA), consistent with the following reactions²⁷:



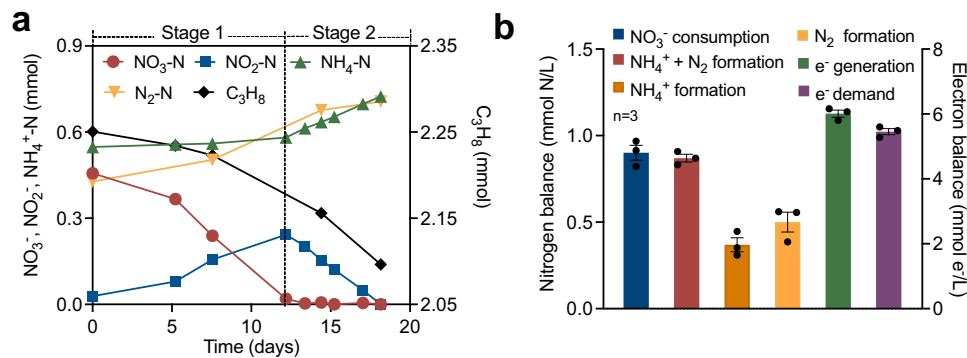


Fig. 2 | Mass balance and electron balance batch tests. a Typical biochemical profile of the systems (started on Day 1050) showing simultaneous nitrate and propane consumption with transitory formation of nitrite, and production of dinitrogen gas and ammonium. Nitrate reduction appeared to occur in two distinct phases. In Stage 1, nitrate was converted to nitrite and dinitrogen gas with

negligible ammonium production; while in Stage 2, both dinitrogen gas and ammonium were generated from accumulated nitrite. **b** Average nitrogen- and electron balances were calculated from the three batch tests (for complete data and calculation see Supplementary Table 1). Error bars represent standard errors. Source data are provided as a Source Data file.

Stoichiometric experiments were conducted both in the parent reactor and in batch incubations seeded with biomass from the parent system, to more accurately establish the nitrogen and electron balances. The nitrate/nitrite reduction appeared to occur in two distinct stages (Fig. 2a). In Stage 1 (before nitrate depletion), nitrate was converted to nitrite and dinitrogen gas with negligible ammonium production. In Stage 2 (after nitrate depletion), both dinitrogen gas and ammonium were generated from nitrite accumulated in Stage 1. The observation that DNRA predominantly occurred when nitrate became limiting is consistent with previous studies^{28–30}. The ratio between nitrate consumption to dinitrogen gas and ammonium production in triplicate batch tests (Fig. 2a, Supplementary Fig. 3) was 1.03 ± 0.05 (Fig. 2b, Supplementary Table 1), suggesting that nitrate was finally fully converted to dinitrogen gas ($57.3 \pm 5.5\%$) and ammonium ($42.7 \pm 5.5\%$). The ratio between electron production (calculated from propane oxidation to CO₂) and electron consumption (nitrate reduction) was 1.10 ± 0.01 (Fig. 2b, Supplementary Table 1), suggesting nitrate reduction was the primary electron sink for propane oxidation.

Characterization of the microbial community of the enrichment

Community profiling with 16S rRNA gene amplicon sequencing revealed that a bacterial phylotype belonging to an unclassified lineage within the phylum Firmicutes was the most abundant population in the bioreactor (20.1% on Day 985, Supplementary Fig. 4), despite being undetectable in the inoculum. To obtain a representative genome for the dominant population, long (Nanopore) and short read (Illumina) metagenomic sequencing (Supplementary Data 1) was performed on biomass from the bioreactor sampled on Day 1040. Assembly and binning of the metagenomic data led to the recovery of 59 near complete genomes ($\geq 70\%$ completeness and $\leq 10\%$ contamination based on CheckM, Supplementary Data 1, Supplementary Fig. 5) including 11 complete circularised genomes (Supplementary Data 1). The most abundant population was classified with the Genome Taxonomy Database (GTDB) to represent a novel order within the Class Symbiobacteriia of the Phylum Firmicutes (22.8% of relative abundance, Supplementary Table 2). We propose the name *Candidatus Alkanivorans nitratreducens* for this bacterium based on its capability in nitrate-dependent propane degradation (see below). The 16S rRNA gene (1536 bp) recovered from the *'Ca. A. nitratreducens'* MAG was identical to the abundant 16S rRNA gene amplicon sequence affiliated to the Firmicutes. The *'Ca. A. nitratreducens'* MAG was complete and circularised with a size of 2.43 Mbp (Supplementary Fig. 6). A genome-based phylogenetic tree showed that the *'Ca. A. nitratreducens'* was phylogenetically distinct from publicly available Symbiobacteriia (Fig. 3a). The

average nucleotide identity (ANI) and amino acid identity (AAI) of the *'Ca. A. nitratreducens'* genome, compared with those of its closest relatives in GTDB, i.e., Symbiobacteriia ZC4RG38, *Symbiobacterium* sp003242675 and *Symbiobacterium thermophilum* (<75.0% and 53.8–55.2% for ANI and AAI, respectively), supports the classification of *'Ca. A. nitratreducens'* as a new order within the class Symbiobacteriia³¹. The 16S rRNA gene tree (Supplementary Fig. 7) also reveals that the *'Ca. A. nitratreducens'* is phylogenetically distant from other classified Symbiobacteriia (<84.1% 16S rRNA gene identity)³¹ and has no close relatives in the Silva database. Three FISH probes (SYMB-1018, SYMB-624 and SYMB-186) were designed and individually applied to the bioreactor biomass to visualise the morphology and spatial arrangement of the *'Ca. A. nitratreducens'* cells. Microscopic examination of the biomass revealed diffuse flocs with the cells appearing to be embedded in an extracellular polymeric substance-like matrix. *'Ca. A. nitratreducens'* appeared as embedded rod shaped cells ($-0.5 \mu\text{m} \times 1.5 \mu\text{m}$) that sometimes formed aggregates (up to $-50 \mu\text{m}$) and were abundant and relatively evenly dispersed throughout the flocs (Fig. 3b and Supplementary Fig. 8). The morphology and spatial arrangement of the cells was consistent for all three probes, giving confidence in their specificity (Supplementary Fig. 8).

Metabolic pathways of *'Ca. A. nitratreducens'*

Annotation of the *'Ca. A. nitratreducens'* MAG identified genes for an ASS complex including two AssD (identical amino acid sequences) and three AssA subunits (89.3–90.7% similarities in amino acid sequences, Supplementary Fig. 9), which mediate the first step of anaerobic activation of SCGAs via fumarate addition^{20,32}. Alignment of *'Ca. A. nitratreducens'* AssA amino acid sequences with homologous sequences in the NCBI database confirmed the conservation of key amino acid residues (Gly828 and Cys489 in AssA1, Gly501 and Cys169 in AssA2, Gly828 and Cys489 in AssA3, Supplementary Fig. 10), which are important for the function of fumarate-adding enzymes³³. Phylogenetic analyses revealed that the AssA and AssD of *'Ca. A. nitratreducens'* are phylogenetically distant from fumarate addition enzymes (AssAD and BssAD) in the NCBI and UniRef databases (Fig. 4c; Supplementary Fig. 11). In addition, the *'Ca. A. nitratreducens'* MAG harbours all genes required for the further degradation of propylsuccinate/*iso*-propylsuccinate, including methylmalonyl-CoA mutase genes (*mcmA*) for carbon-skeleton rearrangement, propionyl-CoA carboxylase genes (*pccB*) for decarboxylation and the key genes for beta-oxidation^{34,35} (Fig. 5; Supplementary Data 2). The acetyl-CoA generated from beta-oxidation may enter the oxidative tricarboxylic acid (TCA) cycle for complete oxidation to CO₂ or for

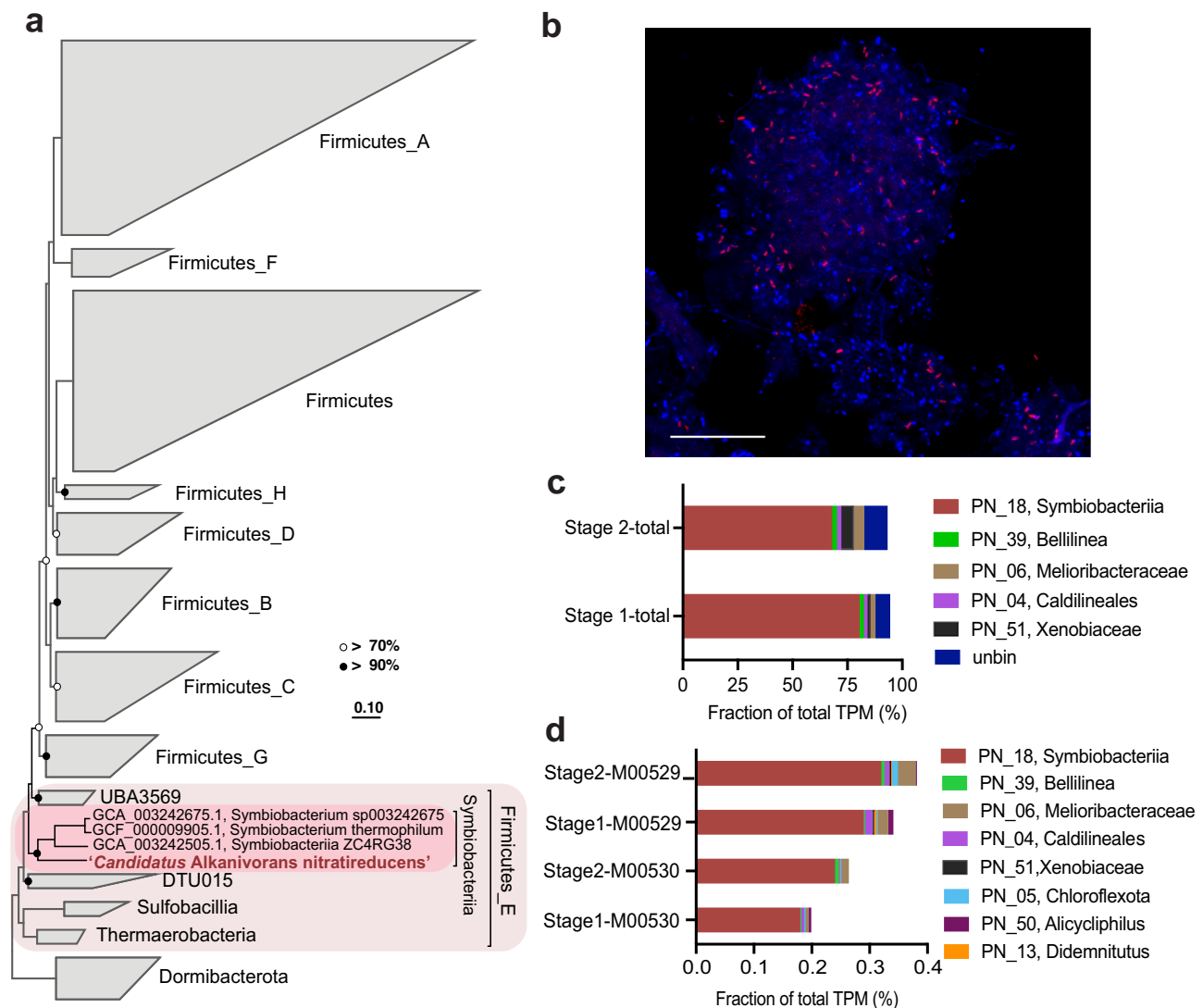


Fig. 3 | Phylogenetic affiliation and a fluorescent micrograph of 'Ca. A. nitratireducens', and relative gene expression profiles for the enrichment culture community. **a** Genome-based phylogenetic tree. The '*Ca. A. nitratireducens*' genome from this study is highlighted in red text. Black and white dots represent >90% and >70% bootstrap values, respectively. The scale bars indicate amino acid substitutions per site. **b** A composite fluorescence micrograph of the enrichment culture hybridized with the SYMB-I018 FISH probe (Cy3, red; targeting '*Ca. A. nitratireducens*' cells appear magenta (blue + red). The scale bar indicates 20 μ m. The representative image was selected based on the visual assessment of six separate

hybridisation experiments. Consistent results were also obtained independently with two additional probes targeting the '*Ca. A. nitratireducens*' population (Supplementary Fig. 8). **c, d** Relative expression of each genome and unbin contigs, and microbial metabolism of interest for the genomes in the bioreactor. The total transcripts per million (TPM) was calculated for each gene. Genome sets with overall expression of total TPM > 1% are shown (c). KEGG annotation was used to identify ORFs coding for denitrification (M00529) and dissimilatory nitrate reduction to ammonium (M00530) pathways (d). Source data are provided as a Source Data file.

regeneration of fumarate for subsequent rounds of propane activation (Fig. 5). The isobutyryl-CoA could be oxidized, via methylmalonic semialdehyde, to propionyl-CoA³⁶, which could be utilized to regenerate fumarate via the methylmalonyl-CoA pathway (Fig. 5). Genes for CO dehydrogenase:Acetyl-CoA synthase (CODH/ACS) and the reverse Wood-Ljungdahl (WL) pathway were identified in '*Ca. A. nitratireducens*', suggesting that terminal oxidation of acetyl-CoA to CO₂ can be mediated by CODH/ACS and stepwise dehydrogenation of the derived C1-units^{37,38} (Fig. 5; Supplementary Data 2; Supplementary Table 3). This WL pathway for CO₂ production is consistent with that proposed for the sulfate-dependent propane degrading *Desulfosarcina aeriohphaga* BuS²¹. Currently, the Class of Symbiobacteriia only includes 3 genomes in the GTDB database and no metabolic models are available for anaerobic propane metabolisms. Therefore, further studies are required to construct metabolic models for '*Ca. A.*

nitratireducens' in order to calculate the carbon flows for TCA and WL pathways and to understand how the cells regulate these two pathways.

Metatranscriptomic and metaproteomic analyses revealed that genes involved in the proposed pathways for complete anaerobic propane oxidation to CO₂ were highly expressed in '*Ca. A. nitratireducens*', and their corresponding gene products were also detected in protein extracts after propane addition (with formyltetrahydrofolate deformylase and formate dehydrogenase as exceptions, Fig. 5; Supplementary Data 2), indicating '*Ca. A. nitratireducens*' played an active role in AOP during both Stage 1 and 2. A search of the entire metagenome library suggested no other populations in the system encoded known genes linked to AOP, including genes for ASS^{20,32} and alkyl-coenzyme M reductase^{22,23}. The relative activity of co-existing microbial populations (collectively accounting

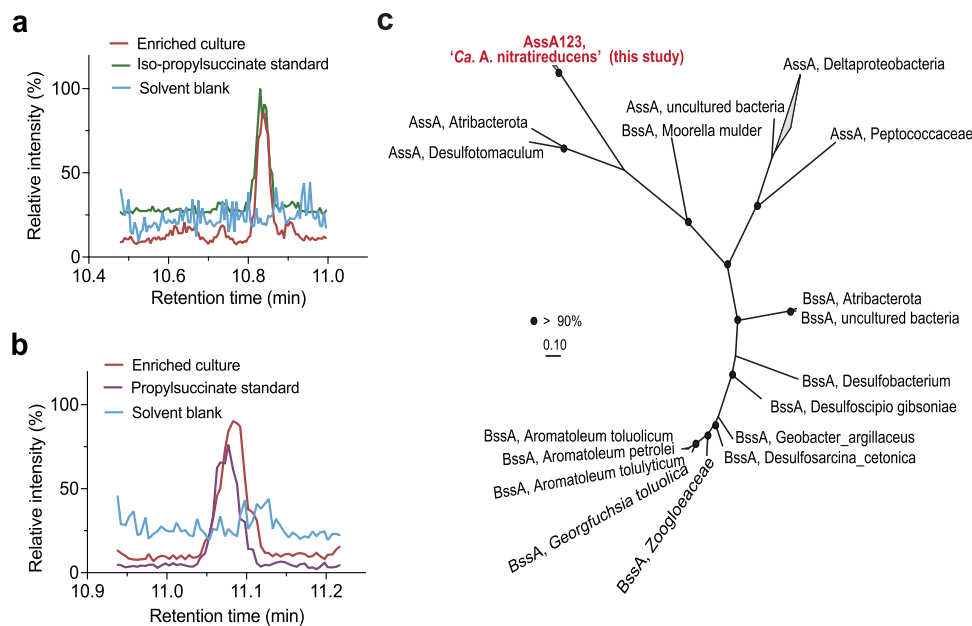


Fig. 4 | Detection of metabolic intermediate in propane oxidation and phylogenetic affiliation of AssA amino acid sequences in ‘*Ca. A. nitratireducens*’ genome. **a** Partial ion chromatograms (ion transition, m/z : 289 > 147.2) of the enriched culture extracts ($n = 3$, taken at various time points) revealed a peak at retention time 10.832 min, matching the peak of the *iso*-propylsuccinate standard. **b** A peak at retention time 11.078 min (ion transition, m/z : 289 > 147.1),

corresponding to the peak from the propylsuccinate standard, was observed for cell extracts from the enriched culture ($n = 3$ at different sampling points). **c** Phylogenetic relationship of ‘*Ca. A. nitratireducens*’ AssA (Red) to other AssA and BssA in the NCBI database. Three AssA subunits (AssA123) found in ‘*Ca. A. nitratireducens*’ MAG formed a separate cluster. Bootstrap values >90% are shown as black dots on branch nodes. Scale bar represents amino acid substitutions per site.

for 14–22% of total transcriptome reads) was also substantially lower than that of ‘*Ca. A. nitratireducens*’ (64–83% of total transcriptome reads, Fig. 3c). These results strongly suggest that ‘*Ca. A. nitratireducens*’ was responsible for AOP in the system.

Cell extracts from the enrichment biomass were analyzed for key metabolites of the activation pathway using ultra-high-sensitivity triple quadrupole mass spectrometry. Total ion chromatograms indicated identical retention time for the propylsuccinate standards and extracted metabolites (Supplementary Fig. 12). Mass peaks corresponding to *iso*-propylsuccinate (m/z : 289 > 147.2) and propylsuccinate (m/z : 289 > 147.1) standards were detected in the cell extracts (Fig. 4a, b). These findings support the hypothesis that ‘*Ca. A. nitratireducens*’ activates propane through homolytic C-H bond cleavage at both primary and secondary carbon atoms, and with addition of fumarate, yields propylsuccinate and *iso*-propylsuccinate. In addition, *iso*-propylsuccinate (5.96 nM) was more abundant than propylsuccinate (2.33 nM) in the culture extracts, suggesting the secondary carbon atom activation generating *iso*-propylsuccinate is the main route of propane oxidation (Fig. 5).

The ‘*Ca. A. nitratireducens*’ MAG also contains all the genes required for DNRA (Fig. 5; Supplementary Table 4), including a nitrate reductase (*napAB*) which catalyses the reduction of nitrate to nitrite, and cytochrome *c* nitrite reductases (*nrfAH*) responsible for reducing generated nitrite to ammonium. Metatranscriptomic results revealed that *napAB* genes encoded by ‘*Ca. A. nitratireducens*’ were more highly expressed in Stage 1 relative to Stage 2, consistent with the higher concentration of nitrate in Stage 1 (Supplementary Fig. 13a). In addition, ‘*Ca. A. nitratireducens*’ *nrfAH* was highly expressed in Stage 2 where the bulk of ammonium was generated (Supplementary Fig. 13b). Moreover, the catalytic subunits of nitrate reductase (NapAB) and cytochrome *c* nitrite reductase (NrfA) were also identified in protein extracts (Fig. 5; Supplementary Table 4). Other members of the community also expressed genes for dissimilatory nitrate reduction pathways (denitrification and DNRA; Fig. 3d), but at substantially lower levels compared to ‘*Ca. A. nitratireducens*’.

The contribution of ‘*Ca. A. nitratireducens*’ to the observed production of dinitrogen gas is not completely clear given the closed representative MAG lacks an identifiable nitric oxide-producing nitrite reductase (*nirS/K*). The MAG has the annotated potential for the last two steps of denitrification; encoding nitric oxide reductase (*norB*) and nitrous oxide reductase (*nosZD*) for the conversion of nitric oxide to dinitrogen gas (Fig. 5; Supplementary Table 4). These genes were highly expressed in both stages and were detected in the protein extracts (Supplementary Table 4), indicating that this microorganism is contributing to the reduction of nitric oxide to dinitrogen gas. These observations suggest that ‘*Ca. A. nitratireducens*’ may utilise a novel gene or novel pathway for nitrite reduction to nitric oxide. Indeed, several other microbes, such as *Bacillus vireti* and methylotrophic bacteria, have been reported to produce nitric oxide even though they do not harbour *nirS/K* genes^{39–41}. It is also possible that other members of the community contribute to the observed denitrification to dinitrogen gas, or the nitrite reduction to nitric oxide. However, the expression of *nirS/K* genes and other denitrification genes was relatively low for all other populations (Fig. 3d), suggesting that ‘*Ca. A. nitratireducens*’ was responsible for the bulk of both the nitrogen- and carbon transformations in the system.

The identification of an anaerobic propane-oxidizing firmicute expands the known phylogenetic diversity of microbial lineages which mediate anaerobic oxidation of SCGAs in the environment, being previously shown for members of the Deltaproteobacteria and archaeal phylum Halobacteriota. To our knowledge, this study is the first to identify a microorganism mediating nitrate-dependent anaerobic propane oxidation (n-DAPO). Given the prevalence of nitrate in various natural and engineered ecosystems, combined with increasing atmospheric emissions of propane due to oil and natural gas production⁴², the previously undescribed n-DAPO process likely occurs in natural environments, representing an overlooked link between global carbon and nitrogen cycling. The newly discovered n-DAPO process may play an important role in reducing the negative

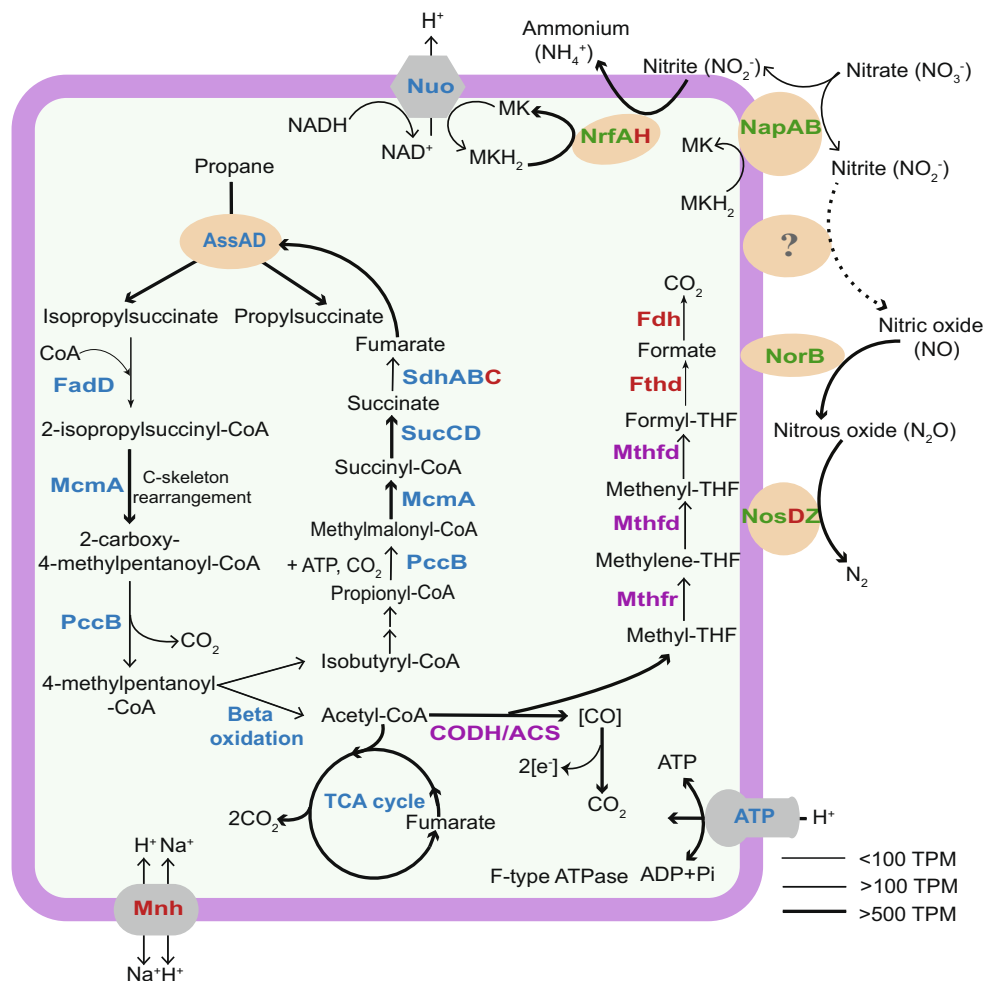


Fig. 5 | Proposed metabolic pathway for anaerobic propane oxidation coupled to nitrate reduction. The ‘*Ca. A. nitratreducens*’ enrichment culture utilized an alkylsuccinate synthase to activate propane to *n*- and *iso*-propylsuccinate. Acetyl-CoA is produced after carbon-skeleton rearrangement, decarboxylation and beta-oxidation. Acetyl-CoA oxidation to CO₂ is catalysed by enzymes involved in the oxidative tricarboxylic acid cycle or reverse Wood–Ljungdahl pathway (purple labels). ‘*Ca. A. nitratreducens*’ harboured all the enzymes involved in denitrification (NapAB, NorB, NosZ, except NirS/K) and DNRA processes (NapAB, NrfAH) (green text). Normalized gene expression for ‘*Ca. A. nitratreducens*’ is indicated as TPM (total transcripts per million). Increasing line thickness shows increasing gene expression values. Enzymes labelled in blue, green, purple and bold text were fully

or partially identified in the protein extracts, while red text indicates enzymes were not detected. Alkylsuccinate synthase, Ass; Long-chain acyl-CoA synthetase, FadD; Methylmalonyl-CoA mutase, Mcm; Propionyl-CoA carboxylase, Pcc; Succinate-CoA ligase, Suc; Succinate dehydrogenase, Sdh; Tricarboxylic acid, TCA; CO dehydrogenase:Acetyl-CoA synthase, CODH/ACS; Methylene-tetrahydrofolate dehydrogenase, Mthfd; methylene-tetrahydrofolate reductase, Mthfr; Formyltetrahydrofolate deformylase, Fthd; Formate dehydrogenase, Fdh; F-type H⁺-transporting ATPase, ATP; NADH-quinone oxidoreductase, Nuo; Multi-component Na⁺ H⁺ antiporter, Mnh; Menaquinol, MKH₂; Menaquinone, MK; Nitrate reductase, Nap; Cytochrome c 552 nitrite reductase, Nrf; Nitric oxide reductase, Nor; Nitrous oxide reductase, Nos.

impact of propane on air quality and on climate, which warrants further investigations. Although propane is a less potent greenhouse gas compared to methane, it can react with the hydroxyl radical, resulting in increased production of ozone^{9,43}. Also, propane contributes to the formation of NO₂ and peroxyacetyl nitrate, two significant air pollutants⁴³. The identification and characterisation of ‘*Ca. A. nitratreducens*’ contributes to a better understanding of the role of microorganisms in regulating SCGA emissions.

Methods

Description of new species

Etymology. Alkanivorans (al.ka.ni.vo’rans. N.L. neut. n. alkanum, alkane; L. pres. part. vorans, devouring; N.L. masc. n. Alkanivorans, an alkane eater). nitratreducens (ni.tri.ta.re.du’cens. N.L. masc. n. nitras (gen. nitratris), nitrate; L. pres. part. reducens, converting to a different state; N.L. part. adj. nitratreducens, reducing nitrate). This name implies an organism capable of consuming propane and reducing nitrogen-related compounds.

Locality. Enriched from a mixture of anaerobic digestion sludge and activated sludge from a wastewater treatment plant in Brisbane, Australia.

Diagnosis. Anaerobic, propane-oxidizing, nitrate-reducing bacteria, typically observed as bacillus shaped cells approximately 0.5 (diameter) × 1.5 μm (length), sometimes forming clusters. Mesophilic in terms of temperature and pH (enriched at 22–25 °C and pH 7–8).

Enrichment bioreactor operation

Without an easy access to sediments in a propane-rich environment, such as deep-sea gas seeps or hot spring sediments, a mixture of approximately 100 mL of anaerobic digestion sludge and 50 mL of activated sludge from a full-scale wastewater treatment plant (Brisbane, Australia) was used as inoculum for the bioreactor enrichment. Wastewater typically contains a wide range of organic substrates enabling the growth of a diverse range of microorganisms. Also, small quantities of propane could also be generated in anaerobic digestion

systems⁴⁴. We hypothesised that some propane oxidizing microorganisms could be present in such systems. The inoculum was incubated in a 2.3 L bioreactor with 1.84 L anoxic synthetic medium prepared as described previously⁴⁵, leaving a headspace of 0.46 L. The propane partial pressure in the headspace was maintained between 0.9 and 1.4 atm by periodically flushed the liquid and headspace with pure propane gas (99.99%, Coregas, Australia). Helium was manually injected into the headspace to pressurize the reactor up to 1.5 atm. Nitrate was pulse-fed to the reactor by manual injection of concentrated stock solution (80 g NO₃⁻-N l⁻¹). The bioreactor was mixed continuously with a magnetic stirrer (IKA, Labtek, Australia) at 400 rpm and incubated at room temperature (22 ± 2 °C). The pH was controlled between 7 and 7.5 by manually adding 1 M anoxic HCl solution. Every 1–3 months, 200 mL of the supernatant was exchanged with fresh synthetic medium. A liquid sample (one mL) was withdrawn 2–3 times per week via the bioreactor sampling port, and 0.22 µm filtered (polyethersulfone filter, Millex, USA) for the measurement of nitrate, nitrite and ammonium. A gas sample (100 µL) was taken from the headspace using a gas-tight syringe (Hamilton, USA) 2–3 times per week for the measurement of propane and dinitrogen gas.

Batch tests for stoichiometric determination

For stoichiometric determination of nitrate reduction and anaerobic propane oxidation, propane and nitrogen concentrations in the headspace of the 2.3 L bioreactor were periodically measured in addition to nitrate, nitrite and ammonium from Day 990 to 1000. In addition, two batch tests were also conducted in 650 mL glass vessels with a subsample of 500 mL biomass anaerobically transferred from the 2.3 L bioreactor (Supplementary Table 5). The biomass was then flushed with argon gas (99.99%, Coregas, Australia) for 20 min to remove dissolved propane in the liquid. Approximately 45 mL propane gas was added to the headspace as the sole electron donor. Enriched cultures without propane, and sterile synthetic medium with propane were set up as controls (Supplementary Table 5). Each batch test was conducted in triplicate.

Isotope labelling batch tests

For the isotope labelling experiments, a subsample of 500 mL biomass from the bioreactor was transferred anaerobically to a 650 mL glass vessel. The biomass was flushed with pure propane gas (99.99%, Coregas, Australia) for 20 min. Approximately 12 mL ¹³C-labelled propane (¹³CH₃¹³CH₂¹³CH₃, 99 atom % ¹³C, Sigma) was injected into the headspace through the septum. Approximately 1 mL nitrate stock solution (10 g N l⁻¹) containing -1% ¹⁵N-labelled sodium nitrate (98 atom % ¹⁵N, Sigma) was added to achieve a concentration of -20 mg N l⁻¹. Using a gas-tight syringe, gas samples were taken periodically from the headspace (Hamilton, USA) and then injected into helium-flushed vials (Exetainer, UK). Liquid samples were collected, filtered (0.22 µm), and stored at -20 °C until analysis for ¹⁵NO₃⁻, ¹⁵NO₂⁻ and ¹⁵NH₄⁺. To quantify the CO₂ produced in the liquid phase, unfiltered samples were injected into Exetainer vials, acidified with 1 M HCl solution, and equilibrated with the headspace for at least 0.5 h before CO₂ determination.

Chemical analysis

Nitrate, nitrite and ammonium concentrations in filtered samples were determined using a Lachat QuickChem8000 flow injection analyzer (Lachat Instrument, Milwaukee, WI). Propane, nitrogen and carbon dioxide concentrations in the headspace were quantified with a gas chromatograph (GC, 7890 A, Agilent, USA) equipped with a thermal conductivity detector and a Shincarbon ST packed column (2 m × 2.0 mm). The gas chromatograph was operated using argon as the carrier gas (flow rate, 28 mL min⁻¹). The oven, injector and detector temperatures were maintained at 220, 250 and 260 °C, respectively. Propane, nitrogen and carbon dioxide concentrations were calculated based on an external standard curve.

Isotopically labelled samples containing nitrate and nitrite were divided into two equal subsamples. For one subsample, nitrate and nitrite ¹⁵N fractions were measured with a Thermo Delta V isotope ratio mass spectrometer (IRMS) after conversion to N₂O⁴⁶. For the other subsample, nitrite was removed using 4% (wt/vol) sulfamic acid in 10% HCl⁴⁷, and the ¹⁵N fraction in the remaining nitrate was measured by IRMS. The fraction of ¹⁵N in nitrite was then calculated using the equation: ¹⁵N fractions in (NO₃⁻ + NO₂⁻) × total amount of (NO₃⁻ + NO₂⁻) = ¹⁵N fraction in NO₃⁻ × total amount of NO₃⁻ + ¹⁵N fraction in NO₂⁻ × total amount of NO₂⁻. Using a microdiffusion method^{48,49}, ammonium was trapped in GF/D filters (Whatman, UK) which were then combusted for isotopic analysis using IRMS. ²⁹N₂, ³⁰N₂, ¹³C-labelled propane and ¹³CO₂ in gas samples were determined with a gas chromatograph (7890 A, Agilent, United States) coupled to a quadrupole mass spectrometer (5957 C inert MSD, Agilent, United States). The gas chromatograph was equipped with a J&W HP-PLOT Q PT column (30 m × 530 µm) and was operated using helium as a carrier gas (flow rate 5.58 mL/min). The oven was maintained at 45 °C for 2 min, and then heated at a rate of 10 °C/min to 60 °C where it was held for 6 min. N₂, CO₂ and C₃H₈ were detected at 70 eV electron impact (EI) using the standard autotune procedure for mass calibration. Acquisition was performed in Total Ion Chromatography (TIC) for identification and in Selected Ion Monitoring (SIM) for monitoring m/z signals at 28, 29 and 30 Da (N₂), 44 and 45 Da (CO₂), 44 and 47 Da (C₃H₈) with a dwell time of 100 ms for each signal. Data processing was performed using the Chemstation program (Agilent, United States).

16 S rRNA gene amplicon sequencing

Biomass samples (10 mL) were taken from the enrichment bioreactor every 2–3 months and pelleted by centrifugation (8000 × g for 10 min) for DNA extraction. DNA was extracted using the FastDNA SPIN for Soil kit (MP Biomedicals, USA) according to the manufacturer's protocol. DNA concentrations were measured using a Nanodrop spectrophotometer (Thermo Fisher Scientific, Wilmington, DE). Amplicon sequencing for the 16 S rRNA genes (V6 to V8 regions) was performed using the universal primer set 926 F (5'-AACTYAAAKGAATTGACGG-3') and 1392 R (5'-ACGGGCGGTGTGTRC-3')⁵⁰ on an Illumina MiSeq platform (Illumina, USA) at the Australian Centre for Ecogenomics (ACE; Brisbane, Australia). Sequencing results were processed using QIIME2⁵⁰.

Metagenomic sequencing and quality control of short- and long-reads

DNA extracted on Day 1040 (for the initial metagenome) and Day 1100 (for the shallow metagenome) was sequenced via short-read paired-end libraries using an Illumina Nextera XT DNA library preparation kit and the NextSeq500 (Illumina, USA) platform at ACE, based on the manufacturer's protocol. Samples for shallow metagenomic sequencing were also taken at the same time as samples for metatranscriptomics sequencing to ensure the microbial community was consistent with the initial metagenome (Supplementary Fig. 14). The libraries generated 149 million and 1 million reads on average for the initial and shallow metagenome, respectively (Supplementary Data 1). Duplicates, adapters and bad quality bases in generated reads were removed using ReadTrim (<https://github.com/jlli6t/ReadTrim>) with parameter "--remove_dups--minlen 100" which internally calls FastQC (<https://www.bioinformatics.babraham.ac.uk/projects/fastqc/>), FastUniq-1.1⁵¹, cutadapt 2.10 and Trimmomatic-0.36⁵².

Biomass from the batch reactor (Day 1120) was also subjected to Nanopore long-read sequencing. DNA was extracted using the Qiagen PowerSoil Pro kit (Qiagen, Germany) and quality-checked using a combination of Qubit 1x dsDNA HS Assay Kit on the Qubit Flex Fluorometer (Thermo Fisher Scientific, Wilmington, DE) and the QIAxcel DNA High Resolution Kit on the QIAxcel Advanced system (Qiagen,

Germany). Library preparation was completed according to the manufacturer's protocol and sequenced on a PromethION (Oxford Nanopore Technologies, USA). Base-calling was performed using Albacore (<https://github.com/Albacore/albacore>), resulting in 73 million reads with quality > Q5. Among them, 12 million reads were longer than 1000 bp with read N50 of 6,135 bp. Adapters were trimmed using Porechop v0.2.4 (<https://github.com/rwrick/Porechop>).

Recovery and evaluation of abundant genomes

Aviary (<https://github.com/rhysnewell/aviary>) was used for hybrid assembly and binning of short- and long-reads, internally calling several different assemblers and binning tools. Results were manually checked using Bandage⁵³. Resulting bins were organized using DAS-Tools 1.1.2⁵⁴. Recovered genomes were further dereplicated using 'dereplicate' workflow in drep-3.2.2⁵⁵ with default settings, resulting in a non-redundant genome set consisting of 59 high-quality genomes. Coverage of genome information and other details were viewed and manually checked using IGV 2.11.1⁵⁶. Completeness and contamination of genomes were checked using CheckM v1.1.3⁵⁷. Quality-trimmed short-reads were mapped to the final MAG set and unbinned contigs using bowtie 2.3.4.3. Mappings with an aligned length ratio over a read <75% or identity of aligned region <97% were removed. Abundance of each MAG was profiled using CoverM 0.6.1 (<https://github.com/wwood/CoverM>) with only quality primary mappings. NGA50 and other genome characteristics were calculated using Python package BioSut (<https://github.com/jlli6t/BioSut>).

Functional annotation

For all MAGs and unbinned contigs, open reading frames (ORFs) were called and primary annotation of genomes was conducted using Prokka 1.14.5⁵⁸ with the domain inferred from GTDB-Tk classification. The KEGG Orthology HMM database (accessed July 2021) was searched against using kofamscan 1.3.0⁵⁹, selecting the top hit for each gene with e-value <1e-10 and maximal F-measure. UniRef100⁶⁰ (accessed March 2020) was indexed with the NCBI taxonomy database and searched against using diamond⁶¹ v2.0.11.149 with 'blastp-sensitive'. The top hit with e-value <1e-5 and identity > 30 was selected and mapped to the KEGG Orthology database. The eggNOG v5 database was searched against using emapper 2.1.5 in diamond mode. Conserved motif(s) present within the predicted genes related to propane oxidation and nitrogen metabolism were further verified using NCBI's conserved domain search⁶². Annotated KO numbers were used for inferring the pathway encoded in each genome. Pathways were identified as 'not expressed' if missed blocks > 75% when total blocks > 5, or missed blocks > 1 when total blocks ≤ 5.

Genome tree construction and classification

A bacterial genome tree was constructed using the Genome Taxonomy Database (GTDB r202) and recovered bacterial genomes with a concatenated set of 120 bacterial-specific conserved marker genes inferred from genomes. Briefly, marker genes in genomes were identified using Prodigal 2.6⁶³ and aligned using HMMER 3.3⁶⁴. Trees were inferred using FastTree 2.1.11⁶⁵ with WAG + GMMMA models. Bootstrapping was performed using GenomeTreeTk v0.1.6 (<https://github.com/dparks1134/GenomeTreeTk>) with 100 times nonparametric bootstrapping. Trees were visualized using ARB 6.0.6⁶⁶ and imported into Adobe Illustrator (Adobe, USA) for further refinement. Classification of genomes was determined using 'classify_wf' workflow in GTDB-Tk v1.5.1⁶⁷.

Phylogenetic analyses of the 16S rRNA gene and alkylsuccinate synthase in '*Ca. A. nitratireducens*'

The 16S rRNA genes were identified in the '*Ca. A. nitratireducens*' MAG and publicly available Symbiobacteria genomes in database. These

genes were compared against the SILVA 138 SSU database. Selected sequences and predicted 16S rRNA gene sequences were dereplicated using cd-hit 4.8.1⁶⁸. In total, 112 16S rRNA sequences were collected and aligned using SSU-align v0.1.1⁶⁹. The phylogenetic tree was inferred using FastTree 2.1.11⁶⁵ with '-gtr-gamma' parameters.

For phylogenetic analyses of AssA in '*Ca. A. nitratireducens*', 24 reference AssA and BssA protein sequences, longer than 700 amino acids (accession numbers of reference sequences are provided in Supplementary Table 6), were downloaded from public databases and aligned using muscle 3.8.31⁷⁰ with parameter '-diags1-maxiters 5'. Gaps in msa were trimmed using trimAl 1.4.1⁷¹. The phylogenetic tree was inferred using FastTree 2.1.11⁶⁵. For construction of both 16S rRNA gene and AssA amino acid trees, bootstrap value calculation and tree visualization were as per the genome tree construction.

Metatranscriptomic sequencing and data analysis

Triplicate batch tests were conducted on Day 1100 in three 650 mL glass vessels with a subsample of 500 mL biomass in each vessel. The nitrate reduction in bioreactors was divided into two stages. In Stage 1, nitrate was mainly converted to nitrite and dinitrogen gas with negligible ammonium production, while in Stage 2 ammonium and dinitrogen gas were both produced. For the co-extraction of total RNA and DNA, 10 mL of an active enriched culture was collected from each batch test in each stage and preserved by adding RNAlater solution (Sigma-Aldrich) and left to stand at room temperature for 1 h. The mixture was then filtered through a sterilized cellulose nitrate filter (0.20 µm; Sartorius; Göttingen, Germany). To capture microorganisms that may pass through the 0.2 µm filter, the filtrate was further concentrated using an Amicon® Ultra Filter (Sigma-Aldrich) with molecular weight cut-off of 100 K. Total RNA and DNA in the concentrated filtrate and cellulose nitrate filter were then extracted by using the RNeasy Powersoil Total RNA kit with the RNeasy Powersoil DNA Elution Kit (Qiagen, Germany) according to the manufacturer's protocols. Trace genomic DNA was removed from the RNA extracts with a Turbo DNA-free kit (Thermo Fisher Scientific, USA) followed by a RNA Clean & Concentrator-5 Kit (Zymo Research, USA). The TruSeq Total RNA Library Prep with Ribo-Zero Plus kit was used for RNA library preparation following the manufacturer's protocol. The library was sequenced on a NextSeq500 (Illumina, USA) platform at ACE (Brisbane, Australia) in 2 × 75 cycles paired-end runs (Table S1).

Generated reads were trimmed using ReadTrim (<https://github.com/jlli6t/ReadTrim>) with parameter "--remove_adap -minlen 60". An rRNA database was constructed from archaeal and bacterial 5S rRNA from 5SRNAdb⁷², SSU database from SILVA⁷³ v138, and LSU database from SILVA v132. Ribosomal RNA-like reads were removed using SortMeRNA 4.2.0⁷⁴ with default settings and database constructed as above. Quality-trimmed reads were mapped to a dereplicated MAGs set and unbinned scaffolds using bowtie2. Alignments with aligned length <95% of read length or identity <97% were removed. Potential DNA contamination of RNA libraries were identified using RNAdir (<https://github.com/jlli6t/RNAdir>), a modified version of dirseq (<https://github.com/wwood/dirseq>). Following, a binomial test was conducted using scipy.stats.binomtest function. Mappings were used for calculation of TPM (total transcripts per million)⁷⁵. Total expression levels of each genome were calculated as the sum of TPM of all coding sequences within each genome.

Protein extraction and metaproteomics

For protein extraction, 10 mL of enrichment culture collected from transcriptomics batch tests was pelleted by centrifugation (18,000 × g, 4 °C), washed with 1 × PBS and stored at -80 °C until analysis. The cell pellets were lysed in 5% sodium dodecyl sulfate (SDS), incubated with 20 mM dithiothreitol (final concentration) at 70 °C for 60 min and then

cooled to room temperature, followed by alkylation with 40 mM iodoacetamide (final concentration) in the dark for 30 min. Afterwards, 1.2% phosphoric acid (final concentration) and six volumes of S-Trap binding buffer (90% methanol, 100 mM final concentration of ammonium bicarbonate, pH 7.1) were added. Total protein was digested in a S-Trap Micro Spin Column (ProtiFi, Huntington, USA) according to the manufacturer's protocol⁷⁶. Briefly, the protein solution was loaded on the S-Trap filter and centrifuged at 4,000 g until all solution passed through. The filter was washed with 150 μ L S-Trap binding buffer three times and digested with 1 μ g sequencing-grade trypsin at 47 °C for 1 h. The digested peptides were sequentially eluted using 40 μ L of 50 mM ammonium bicarbonate, 0.1% aqueous formic acid, 50% acetonitrile and 0.1% formic acid in H₂O. The peptide solutions were dried before being resuspended in 20 μ L of 5% acetonitrile in H₂O. The peptides were analysed by Liquid Chromatography-tandem Mass Spectrometry (LC-MS/MS) using a Dionex Ultimate 3000 RSLCnano-LC system coupled to a Q-Exactive™ H-X Hybrid Quadrupole-Orbitrap™ mass spectrometer (Thermo Scientific™). Raw sequencing data were processed by searching against the annotated metagenomes of '*Ca. A. nitratireducens*' in Thermo Proteome Discoverer (version 2.2.0.388). The identified proteins contained at least 1 unique peptide with a stringency cut-off of false discovery rate (FDR, *q* value) less than 0.05.

Metabolite extraction

For preparation of the metabolite extract, 5 mL of enrichment culture was collected from the bioreactor. The cells were harvested by centrifugation (8000 \times g, 10 min, 4 °C) and then resuspended in 1 mL acetonitrile-methanol-water (4:4:2, vol/vol/vol) mixture in lysing matrix tubes (MP Biomedicals) with glass beads. The cells were lysed using a bead-based homogenizer operated for 5 cycles of reciprocal shaking at low speed (3000 rpm, 50 s) with cooling on ice (15 s) between the homogenization steps. The extracts were separated from cell debris and glass beads by centrifugation at 18,000 g for 10 min at 4 °C and stored at -80 °C until analysis.

Mass spectrometry of standards and cell extracts

The custom synthesized standards (propyl and isopropyl succinate, Best of Chemicals, USA) and cell extracts were dried in a rotational vacuum concentrator (Concentrator Plus, Eppendorf), and then derivatized in 20 μ L methoxyamine chloride (30 mg/mL in pyridine) with continuous mixing for 2 h at 37 °C. *N,O*-bis (trimethylsilyl) trifluoroacetamide (BSTFA, 20 μ L) containing 1% trimethylchlorosilane (TMCS) was then added. Samples were incubated with continuous shaking for 30 min at 37 °C and then analysed using an ultra-high-sensitivity triple quadrupole GC/MS-TQ8050 system (Shimadzu, Japan). The GC system was equipped with an EI ionisation source and operated in multiple reaction monitoring (MRM) mode for the detection of compounds. Helium was used as a carrier gas at a constant flow rate of 1.0 mL/min. One microliter of the derivatised sample was injected into a PTV injector in split mode 1:10 with an injection temperature of 280 °C. Separations were carried out in a DB-5ms column (95% polydimethylsiloxane, 30 m \times 0.25 mm \times 1 μ m) (Agilent JW Scientific). The oven temperature was initially held for 1 min at 120 °C, then increased to 220 °C at a rate of 8 °C/min, and finally increased to 320 °C at 50 °C/min and held for 1 min. The ion source temperature was set at 200 °C. The specific mass spectrometric parameters were tailored for each compound to monitor the fragmentation ions for each analyte (See Supplementary Table 7). Two fragment ions from the EI ion source were nominated and then further fragmented in the collision cell. The three most abundant transients were chosen to monitor. Transient 1 was used as quantifier and the other two as qualifiers.

Fluorescence in situ hybridization (FISH)

FISH was performed essentially as detailed by Daims, et al.⁷⁷. Biomass from the bioreactor was fixed with 4% paraformaldehyde (w/v) and stored in 50% ethanol in PBS at -20 °C. FISH probes were designed using ARB software⁷⁰ against the Silva SSU Ref NR99 database release 138⁷³ including relevant sequences generated from the enrichment bioreactor. In the absence of any related sequences in the database (>92% similarity), the probes were designed against the 16 S sequence of '*Ca. A. nitratireducens*' and care should be taken in their application beyond well characterised systems. Given there are no cultured representatives available for probe validation, three FISH probes were designed to target different sites on the '*Ca. A. nitratireducens*' 16 S rRNA to give higher confidence in their specificity. These included the SYMB-1018 (5'- CCG AAG CCC AGC AAA CTC T - 3'), SYMB-624 (5'- TTC GCA AGC ACT CCC GCA - 3') and SYMB-186 (5'- TCC TCC CGT CCC CAT GC - 3') probes. Unlabelled helper probes⁷⁸ were designed to target the flanking regions of each probe site to increase accessibility to the target site for optimal fluorescent signal (SYMB-1018: H1, 5'- ATT TCT AGA GCG GTC AGG GGA TGT - 3'; H2, 5'- CAC CTG TCT CCC TGT CTG GA - 3'; SYMB-624: H1, 5'- GTT AAG CTG CGG GTT TTC ACT CAC - 3'; H2, 5'- CTG CCC TCA AGC CCA ACA GT - 3'; SYMB-186: H1, 5'- GGC CGT GAG CAT ATC CGG TAT TAG C - 3'; H2a, 5'- GAC CCA TCC CGA AGC AGT AAA CCT T - 3'; H2b, 5'- GAC CCA TCC CGA AGT AGC AAC CCT T - 3'). Helper probes were applied in equimolar amounts with their respective probe. The 5' and 3' ends of the oligonucleotide FISH probes were labelled with the Cy3 fluorophore and were synthesized by Integrated DNA Technologies, Singapore. A higher signal was achieved for these FISH probes with lysozyme pre-treatment of the biomass (0.5 mg ml⁻¹ in 0.05 M EDTA, 0.1 M Tris-HCl, pH 8) for 30 min at room temperature. The Non-EUB nonsense probe was used as a negative hybridization control⁷⁹. DAPI (1 ng/ μ L) staining of cells was performed for 15 min in the dark. The labelled biomass was visualized with a Stellaris5 white light laser confocal microscope (Leica, Germany).

Reporting summary

Further information on research design is available in the Nature Research Reporting Summary linked to this article.

Data availability

Sequencing data are archived in NCBI database under Project number [PRJNA802347](https://doi.org/10.26434/chemrxiv-2022-prjna). All draft genome nucleotide sequences have been submitted to NCBI under accession numbers SAMN25643198 to SAMN25643256. The mass spectrometry proteomics data have been deposited to the ProteomeXchange Consortium via the PRIDE partner repository with the dataset identifier PXD031366. Source data are provided with this paper.

References

1. Joye, S. B. The geology and biogeochemistry of hydrocarbon seeps. *Annu. Rev. Earth Planet. Sci.* **48**, 205–231 (2020).
2. Etiope, G., Feyzullayev, A. & Baciu, C. L. Terrestrial methane seeps and mud volcanoes: a global perspective of gas origin. *Mar. Pet. Geol.* **26**, 333–344 (2009).
3. Mastalerz, V., De Lange, G. J. & Dählmann, A. Differential aerobic and anaerobic oxidation of hydrocarbon gases discharged at mud volcanoes in the Nile deep-sea fan. *Geochim. Cosmochim. Acta* **73**, 3849–3863 (2009).
4. Musat, F. The anaerobic degradation of gaseous, nonmethane alkanes—From in situ processes to microorganisms. *Comput. Struct. Biotechnol. J.* **13**, 222–228 (2015).
5. Gilbert, A. et al. Intramolecular isotopic evidence for bacterial oxidation of propane in subsurface natural gas reservoirs. *Proc. Natl Acad. Sci. USA* **116**, 6653–6658 (2019).

6. Orphan, V. J., House, C. H., Hinrichs, K.-U., McKeegan, K. D. & DeLong, E. F. Methane-consuming archaea revealed by directly coupled isotopic and phylogenetic analysis. *Science* **293**, 484–487 (2001).
7. Knittel, K. & Boetius, A. Anaerobic oxidation of methane: progress with an unknown process. *Annu. Rev. Microbiol.* **63**, 311–334 (2009).
8. Singh, R., Guzman, M. S. & Bose, A. Anaerobic oxidation of ethane, propane, and butane by marine microbes: a mini review. *Front. microbiol.* **8**, 2056 (2017).
9. Saito, T., Yokouchi, Y. & Kawamura, K. Distributions of C₂–C₆ hydrocarbons over the western North Pacific and eastern Indian Ocean. *Atmos. Environ.* **34**, 4373–4381 (2000).
10. Pozzer, A. et al. Observed and simulated global distribution and budget of atmospheric C₂–C₅ alkanes. *Atmospheric Chem. Phys.* **10**, 4403–4422 (2010).
11. Boetius, A. et al. A marine microbial consortium apparently mediating anaerobic oxidation of methane. *Nature* **407**, 623–626 (2000).
12. Wegener, G., Krukenberg, V., Riedel, D., Tegetmeyer, H. E. & Boetius, A. Intercellular wiring enables electron transfer between methanotrophic archaea and bacteria. *Nature* **526**, 587–590 (2015).
13. Haroon, M. F. et al. Anaerobic oxidation of methane coupled to nitrate reduction in a novel archaeal lineage. *Nature* **500**, 567–570 (2013).
14. Leu, A. O. et al. Anaerobic methane oxidation coupled to manganese reduction by members of the Methanoperedenaceae. *ISME J.* **14**, 1030–1041 (2020).
15. Cai, C. et al. A methanotrophic archaeon couples anaerobic oxidation of methane to Fe(III) reduction. *ISME J.* **12**, 1929–1939 (2018).
16. Ettwig, K. F. et al. Archaea catalyze iron-dependent anaerobic oxidation of methane. *Proc. Natl Acad. Sci. USA* **113**, 12792–12796 (2016).
17. Ettwig, K. F. et al. Nitrite-driven anaerobic methane oxidation by oxygenic bacteria. *Nature* **464**, 543–548 (2010).
18. Widdel, F. & Musat, F. In *Handbook of Hydrocarbon and Lipid Microbiology* 981–1009 (Springer, 2010).
19. Ettwig, K. F. Nitrite-dependent methane oxidation. Diss. Radboud University Nijmegen (2010).
20. Kniemeyer, O. et al. Anaerobic oxidation of short-chain hydrocarbons by marine sulphate-reducing bacteria. *Nature* **449**, 898 (2007).
21. Chen, S.-C. et al. Genome and proteome analyses show the gaseous alkane degrader *Desulfosarcina* sp. strain BuS5 as an extreme metabolic specialist. *Environ. Microbiol.* **24**, 964–1976 (2022).
22. Chen, S.-C. et al. Anaerobic oxidation of ethane by archaea from a marine hydrocarbon seep. *Nature* **568**, 108–111 (2019).
23. Laso-Pérez, R. et al. Thermophilic archaea activate butane via alkyl-coenzyme M formation. *Nature* **539**, 396–401 (2016).
24. Hahn, C. J. et al. “*Candidatus Ethanoperedens*,” a thermophilic genus of archaea mediating the anaerobic oxidation of ethane. *MBio* **11**, e00600-20 (2020).
25. Jaekel, U. et al. Anaerobic degradation of propane and butane by sulfate-reducing bacteria enriched from marine hydrocarbon cold seeps. *ISME J.* **7**, 885–895 (2013).
26. Addiscott, T. M. *Nitrate, agriculture and the environment*. (CABI, 2005).
27. John, A. D. Lange’s Handbook of Chemistry. McGraw-Hill Book Co., New York, 1979.
28. Burgin, A. J. & Hamilton, S. K. Have we overemphasized the role of denitrification in aquatic ecosystems? A review of nitrate removal pathways. *Front. Ecol. Environ.* **5**, 89–96 (2007).
29. Rütting, T., Boeckx, P., Müller, C. & Klemedtsson, L. Assessment of the importance of dissimilatory nitrate reduction to ammonium for the terrestrial nitrogen cycle. *Biogeosciences* **8**, 1779–1791 (2011).
30. Van Den Berg, E. M., Van Dongen, U., Abbas, B. & Van Loosdrecht, M. C. Enrichment of DNRA bacteria in a continuous culture. *ISME J.* **9**, 2153–2161 (2015).
31. Konstantinidis, K., Rosselló-Móra, R. & Amann, R. Uncultivated microbes in need of their own taxonomy. *ISME J.* **11**, 2399–2406 (2017).
32. Callaghan, A. V., Wawrik, B., Chadhain, S. M. N., Young, L. Y. & Zylstra, G. J. Anaerobic alkane-degrading strain AK-01 contains two alkylsuccinate synthase genes. *Biochem. Biophys. Res. Commun.* **366**, 142–148 (2008).
33. Heider, J. et al. Structure and function of benzylsuccinate synthase and related fumarate-adding glycy radical enzymes. *J. Mol. Microbiol. Biotechnol.* **26**, 29–44 (2016).
34. Callaghan, A. V. et al. The genome sequence of *Desulfatibacillum alkenivorans* AK-01: a blueprint for anaerobic alkane oxidation. *Environ. Microbiol.* **14**, 101–113 (2012).
35. Liu, Y.-F. et al. Anaerobic hydrocarbon degradation in candidate phylum ‘Atribacteria’(JS1) inferred from genomics. *ISME J.* **13**, 2377–2390 (2019).
36. Stieb, M. & Schink, B. Anaerobic degradation of isobutyrate by methanogenic enrichment cultures and by a *Desulfococcus multivorans* strain. *Arch. Microbiol.* **151**, 126–132 (1989).
37. Adam, P. S., Borrel, G. & Grimaldo, S. Evolutionary history of carbon monoxide dehydrogenase/acetyl-CoA synthase, one of the oldest enzymatic complexes. *Proc. Natl. Acad. Sci. USA* **115**, E1166–E1173 (2018).
38. Schauder, R., Eikmanns, B., Thauer, R. K., Widdel, F. & Fuchs, G. Acetate oxidation to CO₂ in anaerobic bacteria via a novel pathway not involving reactions of the citric acid cycle. *Arch. Microbiol.* **145**, 162–172 (1986).
39. Mania, D., Heylen, K., van Spanning, R. J. M. & Frostegård, Å. The nitrate-ammonifying and nosZ-carrying bacterium *B. acillus vireti* is a potent source and sink for nitric and nitrous oxide under high nitrate conditions. *Environ. Microbiol.* **16**, 3196–3210 (2014).
40. Mauffrey, F., Cucaita, A., Constant, P. & Villemur, R. Denitrifying metabolism of the methylotrophic marine bacterium *Methylophaga nitratireducens* strain JAM1. *PeerJ* **5**, 2167–8359 (2017).
41. Onley, J. R., Ahsan, S., Sanford, R. A. & Löffler, F. E. Denitrification by *Anaeromyxobacter dehalogenans*, a common soil bacterium lacking the nitrite reductase genes nirS and nirK. *Appl. Environ. Microbiol.* **84**, e01985–01917 (2018).
42. Helmig, D. et al. Reversal of global atmospheric ethane and propane trends largely due to US oil and natural gas production. *Nat. Geosci.* **9**, 490–495 (2016).
43. Dalsøren, S. B. et al. Discrepancy between simulated and observed ethane and propane levels explained by underestimated fossil emissions. *Nat. Geosci.* **11**, 178–184 (2018).
44. Gollakota, K. G. & Jayalakshmi, B. Biogas (natural gas?) production by anaerobic digestion of oil cake by a mixed culture isolated from cow dung. *Biochemical Biophysical Res. Commun.* **110**, 32–35 (1983).
45. Ettwig, K. F., van Alen, T., van de Pas-Schoonen, K. T., Jetten, M. S. & Strous, M. Enrichment and molecular detection of denitrifying methanotrophic bacteria of the NC10 phylum. *Appl. Environ. Microbiol.* **75**, 3656–3662 (2009).
46. Sigman, D. M. et al. A bacterial method for the nitrogen isotopic analysis of nitrate in seawater and freshwater. *Anal. Chem.* **73**, 4145–4153 (2001).
47. Granger, J. & Sigman, D. M. Removal of nitrite with sulfamic acid for nitrate N and O isotope analysis with the denitrifier method. *Rapid Commun. Mass Spectrom.* **23**, 3753–3762 (2009).
48. Zhang, S., Fang, Y. & Xi, D. Adaptation of micro-diffusion method for the analysis of 15N natural abundance of ammonium in samples

- with small volume. *Rapid Commun. Mass Spectrom.* **29**, 1297–1306 (2015).
49. Holmes, R. M., McClelland, J. W., Sigman, D. M., Fry, B. & Peterson, B. J. Measuring 15N-NH_4^+ in marine, estuarine and fresh waters: an adaptation of the ammonia diffusion method for samples with low ammonium concentrations. *Mar. Chem.* **60**, 235–243 (1998).
50. Wu, M., Luo, J.-H., Hu, S., Yuan, Z. & Guo, J. Perchlorate bio-reduction in a methane-based membrane biofilm reactor in the presence and absence of oxygen. *Water Res.* **157**, 572–578 (2019).
51. Xu, H. et al. FastUniq: a fast de novo duplicates removal tool for paired short reads. *PLoS One* **7**, e52249 (2012).
52. Bolger, A. M., Lohse, M. & Usadel, B. Trimmomatic: a flexible trimmer for Illumina sequence data. *Bioinformatics* **30**, 2114–2120 (2014).
53. Wick, R. R., Schultz, M. B., Zobel, J. & Holt, K. E. Bandage: interactive visualization of de novo genome assemblies. *Bioinformatics* **31**, 3350–3352 (2015).
54. Sieber, C. M. K. et al. Recovery of genomes from metagenomes via a dereplication, aggregation and scoring strategy. *Nat. Microbiol.* **3**, 836–843 (2018).
55. Olm, M. R., Brown, C. T., Brooks, B. & Banfield, J. F. dRep: a tool for fast and accurate genomic comparisons that enables improved genome recovery from metagenomes through de-replication. *ISME J.* **11**, 2864–2868 (2017).
56. Robinson, J. T. et al. Integrative genomics viewer. *Nat. Biotechnol.* **29**, 24–26 (2011).
57. Parks, D. H., Imelfort, M., Skennerton, C. T., Hugenholtz, P. & Tyson, G. W. CheckM: assessing the quality of microbial genomes recovered from isolates, single cells, and metagenomes. *Genome Res.* **25**, 1043–1055 (2015).
58. Seemann, T. Prokka: rapid prokaryotic genome annotation. *Bioinformatics* **30**, 2068–2069 (2014).
59. Aramaki, T. et al. KofamKOALA: KEGG ortholog assignment based on profile HMM and adaptive score threshold. *Bioinformatics* **36**, 2251–2252 (2019).
60. Suzek, B. E., Huang, H., McGarvey, P., Mazumder, R. & Wu, C. H. UniRef: comprehensive and non-redundant UniProt reference clusters. *Bioinformatics* **23**, 1282–1288 (2007).
61. Buchfink, B., Xie, C. & Huson, D. H. Fast and sensitive protein alignment using DIAMOND. *Nat. Methods* **12**, 59–60 (2015).
62. Marchler-Bauer, A. & Bryant, S. H. CD-Search: protein domain annotations on the fly. *Nucleic Acids Res.* **32**, W327–W331 (2004).
63. Hyatt, D. et al. Prodigal: prokaryotic gene recognition and translation initiation site identification. *BMC Bioinforma.* **11**, 119 (2010).
64. Eddy, S. R. Accelerated Profile HMM Searches. *PLoS Comput. Biol.* **7**, e1002195 (2011).
65. Price, M. N., Dehal, P. S. & Arkin, A. P. FastTree 2-approximately maximum-likelihood trees for large alignments. *PLoS One* **5**, e9490 (2010).
66. Ludwig, W. et al. ARB: a software environment for sequence data. *Nucleic Acids Res.* **32**, 1363–1371 (2004).
67. Chaumeil, P. A., Mussig, A. J., Hugenholtz, P. & Parks, D. H. GTDB-Tk: a toolkit to classify genomes with the Genome Taxonomy Database. *Bioinformatics* **36**, 1925–1927 (2019).
68. Fu, L., Niu, B., Zhu, Z., Wu, S. & Li, W. CD-HIT: accelerated for clustering the next-generation sequencing data. *Bioinformatics* **28**, 3150–3152 (2012).
69. Nawrocki, E. P. Structural RNA homology search and alignment using covariance models. (Washington University in St. Louis, 2009).
70. Edgar, R. C. MUSCLE: multiple sequence alignment with high accuracy and high throughput. *Nucleic Acids Res.* **32**, 1792–1797 (2004).
71. Capella-Gutierrez, S., Silla-Martinez, J. M. & Gabaldon, T. trimAl: a tool for automated alignment trimming in large-scale phylogenetic analyses. *Bioinformatics* **25**, 1972–1973 (2009).
72. Szymanski, M., Zielezinski, A., Barciszewski, J., Erdmann, V. A. & Karlowski, W. M. 5SRNAdb: an information resource for 5S ribosomal RNAs. *Nucleic Acids Res.* **44**, D180–D183 (2016).
73. Quast, C. et al. The SILVA ribosomal RNA gene database project: improved data processing and web-based tools. *Nucleic Acids Res.* **41**, D590–D596 (2013).
74. Kopylova, E., Noe, L. & Touzet, H. SortMeRNA: fast and accurate filtering of ribosomal RNAs in metatranscriptomic data. *Bioinformatics* **28**, 3211–3217 (2012).
75. Wagner, G. P., Kin, K. & Lynch, V. J. Measurement of mRNA abundance using RNA-seq data: RPKM measure is inconsistent among samples. *Theor. Biosci.* **131**, 281–285 (2012).
76. HaileMariam, M. et al. S-Trap, an ultrafast sample-preparation approach for shotgun proteomics. *J. Proteome Res.* **17**, 2917–2924 (2018).
77. Daims, H., Stoecker, K. & Wagner, M. In *Molecular Microbial Ecology* 208–228 (Taylor & Francis, 2004).
78. Fuchs, B. M., Glöckner, F. O., Wulf, J. & Amann, R. Unlabeled helper oligonucleotides increase the in situ accessibility to 16S rRNA of fluorescently labeled oligonucleotide probes. *Appl. Environ. Microbiol.* **66**, 3603–3607 (2000).
79. Wallner, G., Amann, R. & Beisker, W. Optimizing fluorescent in situ hybridization with rRNA-targeted oligonucleotide probes for flow cytometric identification of microorganisms. *Cytom.,: j. Int. Soc. Anal. Cytol.* **14**, 136–143 (1993).

Acknowledgements

We acknowledge A. Oren (The Hebrew University of Jerusalem) for suggestions on the naming of ‘Ca. A. nitratireducens’, G. Talbo and L. Liu for help with protein extraction and proteomics data analysis, Y. Wang and C. Lai for assistance with bioreactor operation, X. Zhang and S. Hu for maintenance of gas chromatograph, N. Clayton, N. Dawson and J. Li for chemical analyses, A. Tabrett and A. McInnes for help with optimising the FISH probes, and E. Larsen for assistance with editing. J.L. is supported by UQ Research Training Scholarship. J.G., S.M. and G.T. are supported by Australian Research Council (ARC) Future Fellowships FT170100196, FT190100211 and FT170100070, respectively. Z.Y. is supported by ARC Australian Laureate Fellowship (FL170100086).

Author contributions

J.G. conceived the study. M.W., J.G. and S.M. planned the experiments. M.W. enriched the microorganisms in the bioreactor and performed mass and electron balance and isotope labelling experiments. D.E. conducted the isotope nitrogen measurements. T.S. set up methods for the isotope carbon and metabolite analyses. S.M. designed FISH probes and conducted FISH microscopy. M.W. performed the sampling, preservation, DNA, RNA and protein extractions for metagenomics, metatranscriptomics and metaproteomics sequencing. M.W., J.G. and Z.Y. performed the process data analysis. J.L. A.L., M.W., G.T., S.M. and J.G. performed the microbial community analysis and the bioinformatics analysis. M.W., J.L. Z.Y., S.M. and J.G. wrote the manuscript in consultation with all other authors.

Competing interests

The authors declare no competing interests.

Additional information

Supplementary information The online version contains supplementary material available at <https://doi.org/10.1038/s41467-022-33872-y>.

Correspondence and requests for materials should be addressed to Simon J. McIlroy or Jianhua Guo.

Peer review information *Nature Communications* thanks Florin Musat and the other, anonymous, reviewer for their contribution to the peer review of this work.

Reprints and permission information is available at <http://www.nature.com/reprints>

Publisher's note Springer Nature remains neutral with regard to jurisdictional claims in published maps and institutional affiliations.

Open Access This article is licensed under a Creative Commons Attribution 4.0 International License, which permits use, sharing, adaptation, distribution and reproduction in any medium or format, as long as you give appropriate credit to the original author(s) and the source, provide a link to the Creative Commons license, and indicate if changes were made. The images or other third party material in this article are included in the article's Creative Commons license, unless indicated otherwise in a credit line to the material. If material is not included in the article's Creative Commons license and your intended use is not permitted by statutory regulation or exceeds the permitted use, you will need to obtain permission directly from the copyright holder. To view a copy of this license, visit <http://creativecommons.org/licenses/by/4.0/>.

© The Author(s) 2022

¹Australian Centre for Water and Environmental Biotechnology, Faculty of Engineering, Architecture and Information Technology, The University of Queensland, St Lucia, QLD, Australia. ²Centre for Microbiome Research, School of Biomedical Sciences, Queensland University of Technology (QUT), Translational Research Institute, Woolloongabba, QLD, Australia. ³Centre for Coastal Biogeochemistry Research, Faculty of Science and Engineering, Southern Cross University, Lismore, NSW, Australia. ⁴Metabolomics Australia (Queensland Node), Australian Institute for Bioengineering and Nanotechnology, The University of Queensland, St Lucia, QLD 4072, Australia. ⁵These authors contributed equally: Mengxiong Wu, Jie Li.

✉ e-mail: simon.mcilroy@qut.edu.au; jianhua.guo@uq.edu.au